

**INSTITUT D'AERONOMIE SPATIALE DE BELGIQUE**

**3 - Avenue Circulaire**

**B - 1180 BRUXELLES**

**AERONOMICA ACTA**

**A - N°95 - 1972**

**On an ion exosphere with asymmetric velocity distribution**

**by J. LEMAIRE and M. SCHERER**

**BELGISCH INSTITUUT VOOR RUIMTE-AERONOMIE**

**3 - Ringlaan**

**B - 1180 BRUSSEL**

## **FOREWORD**

**This paper will be published in the Physics of Fluids.**

## **AVANT-PROPOS**

**Ce travail sera publié dans The Physics of Fluids.**

## **VOORWOORD**

**Deze tekst zal verschijnen in The Physics of Fluids.**

## **VORWORT**

**Dieser Text wird in The Physics of Fluids herausgegeben werden.**

# ON AN ION EXOSPHERE WITH ASYMMETRIC VELOCITY DISTRIBUTION

by

J. LEMAIRE and M. SCHERER

## *Abstract*

The number density, the particle flux, the momentum fluxes and the energy flux are calculated in a model ion-exosphere with an open magnetic field, for an asymmetric Maxwellian velocity distribution (i.e.  $\sim \exp[-\beta(\vec{v}-\vec{u})^2]$ ). Numerical calculations for the polar ionosphere of the earth show that this asymmetry does not qualitatively affect the results obtained with a symmetric velocity distribution function ( $u = 0$ ), i.e., the protons are accelerated outwards and escape with a supersonic flow speed.

## *Résumé*

La densité, le flux de particules, les flux d'impulsion et d'énergie sont calculés dans un modèle d'exosphère ionique pour une distribution des vitesses asymétrique et Maxwellienne (c.à.d.  $\sim \exp[-\beta(\vec{v}-\vec{u})^2]$ ). L'application à l'ionosphère polaire montre que cette asymétrie n'affecte pas qualitativement les résultats obtenus avec une distribution des vitesses symétrique ( $u = 0$ ), les protons sont accélérés vers l'extérieur et s'échappent avec une vitesse supersonique.

### *Samenvatting*

De deeltjes dichtheid, de deeltjes flux, de momenten flux en de energie flux worden berekend voor een asymmetrische Maxwell snelheidsverdeling [ $\sim \exp - \beta(\vec{v} - \vec{u})^2$ ] in een eenvoudig model voor een ionaire exosfeer met een open magneetveld. Numerieke berekeningen voor de polaire ionosfeer van de aarde tonen aan dat zulke asymmetrie de resultaten bekomen met een symmetrische snelheidsverdeling ( $u = 0$ ) kwalitatief niet wijzigt: de protonen worden versneld naar buiten uit en ontsnappen met een supersonische snelheid.

### *Zusammenfassung*

Die Dichte, die Ausflüsse der Teilchen, der Impulsion und der Energie sind in einem Ionenexosphärischen Modell mit offene magnetische Feldlinien, berechnet worden, für eine asymmetrische und Maxwellische Distribution (d.h.  $\sim \exp[-\beta(\vec{v} - \vec{u})^2]$ ). Es wird gezeigt dass im Falle der polaren Ionosphäre diese Asymmetrie die Resultate die man für eine symmetrische Distribution ( $u = 0$ ) erhält, nicht qualitativ verändert: die Protonen sind nach Aussen beschleunigt und entfliehen aus der Ionosphäre mit einer überschallgeschwindigkeit.

## I. INTRODUCTION

Recently, Lemaire and Scherer <sup>1</sup>, determined the number density, the flux, the pressure tensor components, and the energy flux in a simple model ion-exosphere of a nonrotating planet with an open magnetic field. They used the following assumptions: (a) The exosphere is separated from the barosphere or collision-dominated region by a sharply defined surface called the baropause; (b) The magnetic field strength is a monotonic decreasing function along a field line, reaching a minimum at infinity; (c) In the exosphere the particle trajectories can be determined by the well-known non relativistic guiding-center approximation, and the particle drift across magnetic field lines can be neglected. Under these assumptions the exospheric particles can be classified into four conventional classes: (1) the ballistic particles which emerge from the barosphere but can not escape, (2) the escaping particles which leave the barosphere and are lost in the interplanetary space, (3) the trapped particles which have two mirror points in the exosphere between which they bounce continuously up and down, and (4) the incoming particles which originate from the outermost regions.

Assuming a symmetric Maxwellian velocity distribution function at the baropause (i.e.  $\sim \exp(-\beta v^2)$ ), the velocity distribution in the collision-free exosphere was calculated by applying Liouville's theorem. In the special case of a vanishing magnetic field at infinity, Lemaire and Scherer <sup>1,2</sup> applied this model ion-exosphere to the polar topside ionosphere of the Earth. For an ( $O^+ - H^+ - e$ ) exosphere they found that the thermal electrons and oxygen ions are decelerated by the combined effect of the induced electric field and the gravitational field. The protons, however, are accelerated outward and rapidly reach a supersonic flow speed. In this paper the formulae obtained previously will be generalized by assuming that the velocity distribution function of the particles at the baropause is Maxwellian but asymmetric. This seems to be a more realistic model for application to the terrestrial polar ionosphere since it has been found that the effusion velocity of the protons is nearly sonic at the baropause <sup>2</sup> and other recent investigations <sup>3-8</sup> have also shown that a supersonic outward flow of  $H^+$  exists in this region. Numerical calculations, however, show that the mean features obtained with a symmetric Maxwellian distribution function remain. In Sec. II we determine the velocity distribution in the exosphere. In Sec. III we calculate the number density and particle flux, the pressure tensor components and the energy flux; and in Sec. IV we finally numerically investigate the influence of an asymmetry in the velocity distribution function, for a model ion-exosphere of the Earth.

For a detailed study of the equations of motion and the classification of the exospheric particles we refer to a previous paper <sup>1</sup>.

## II. THE VELOCITY DISTRIBUTION

If the effusion velocity of a constituent is comparable to the thermal speed of this species, the velocity distribution of these particles is highly asymmetric in the direction parallel to the flow. Therefore, we assume that for particles emerging from the barosphere, the actual velocity distribution function at the baropause can be approximated by

$$f(\vec{r}_0, \vec{v}) = n_0 \left( \frac{m}{2\pi k T_0} \right)^{3/2} \exp \left( - \frac{m}{2k T_0} (\vec{v} - \vec{u})^2 \right), \quad (1)$$

where  $k$  is the Boltzmann constant,  $m$  is the mass of particles,  $r_0$  is the radial distance of the baropause,  $n_0$  and  $T_0$  are constants, and  $\vec{u}$  represents a velocity vector parallel to the magnetic field  $\vec{B}(\vec{r}_0)$ . These parameters are chosen to obtain at the baropause respectively a given number density  $n(\vec{r}_0)$ , temperature  $T(\vec{r}_0)$ , and bulk velocity  $w(\vec{r}_0)$  which is the ratio of the escape flux  $F(\vec{r}_0)$  to  $n(\vec{r}_0)$ . Since the moments of the velocity distribution are function of the parameters  $n_0$ ,  $T_0$  and  $u$  (see Sec. III), the relation between  $n_0$  and  $n(\vec{r}_0)$ ,  $T_0$  and  $T(\vec{r}_0)$ ,  $u$  and  $w(\vec{r}_0)$  can be determined.

Even in the case of a symmetric velocity distribution function ( $u = 0$ ) the effusion velocity at the baropause is not zero. This is a consequence of the truncation of the velocity distribution to exclude the incoming particles. The actual velocity distribution at the baropause can be quite different from (1) or any linear combination of Maxwellian's. It will always be possible, however, to determine the parameters  $n_0$ ,  $T_0$ ,  $u, \dots$ ; in order to fit a fixed number of moments of the approximated velocity distribution to the corresponding moments of the actual distribution.

The velocity distribution in the exosphere is obtained by solving Vlasov's equation subject to the boundary condition (1)

$$f(\vec{r}, \vec{v}) = n_0 \left( \frac{m}{2\pi k T_0} \right)^{3/2} \exp \left( - \frac{m}{2k T_0} [v^2 + R + u^2 - 2u(v^2 + R - \eta^{-1} v^2 \sin^2 \theta)^{1/2}] \right). \quad (2)$$

where R is defined by

$$R = -2\psi [1 + a - (1 + \beta)y] , \quad y = r_0/r \quad (3)$$

$$a = Ze \varphi_0(\vec{r}_0)/m\psi, \quad (4)$$

$$\beta = Ze \varphi_0(\vec{r})/m\psi,$$

and where  $\theta$  is the pitch angle of the particle with mass  $m$ , charge  $Ze$ , and velocity  $v$ ;  $\psi$  is the gravitational potential at the baropause level,  $\varphi_0$  is the electrostatic potential due to the small charge separation, and  $\eta = B(\vec{r})/B(\vec{r}_0)$  is the ratio of the magnetic field strength at the radial distance  $r$  to the magnetic field strength at the baropause.

### III. MOMENTS OF THE VELOCITY DISTRIBUTION

In this section we determine the formulae for the number density, the particle flux parallel to the magnetic field, the parallel and perpendicular momentum fluxes, and the energy flux, for particles with velocity distribution (2). These macroscopic quantities are defined as the different moments of the velocity distribution in a previous paper<sup>1</sup>, and we will use the same notations here.

#### A. Ballistic Particles

It can be shown<sup>(1)</sup> that the ballistic particles have a positive potential energy  $mR/2$  and that the velocity space corresponding to this class of particles is given by :

$$\begin{aligned} 0 \leq v \leq v_b & , \quad 0 \leq \theta \leq \pi , \quad 0 \leq \varphi < 2\pi \quad ; \\ v_b \leq v \leq v_\infty & , \quad \left\{ \begin{array}{l} 0 \leq \theta \leq \theta_m , \\ \pi - \theta_m \leq \theta \leq \pi \end{array} \right. \quad 0 \leq \varphi < 2\pi \quad ; \quad (5) \\ v_\infty \leq v \leq v_c & , \quad \left\{ \begin{array}{l} \theta'_m \leq \theta \leq \theta_m \\ \pi - \theta_m \leq \theta \leq \pi - \theta'_m \end{array} \right. \quad 0 \leq \varphi < 2\pi \quad ; \end{aligned}$$

with

$$v_b^2 = \eta R / (1 - \eta) \quad ,$$

$$v_\infty^2 = -2\psi (1 + \beta)y \quad ,$$

$$v_c^2 = -2\psi a(1 + a)/(1 - a) - 2\psi (1 + \beta)y \quad ,$$

$$\theta_m = \arcsin \left[ \eta^{1/2} (1 + R/v^2)^{1/2} \right] \quad , \quad (6)$$

$$\theta'_m = \arcsin \left[ \mu^{1/2} (1 - v_\infty^2/v^2)^{1/2} \right] \quad ,$$

$$a = B(\infty)/B(\vec{r}_0) \quad ,$$

$$\mu = \eta/a = B(\vec{r})/B(\infty)$$

The angle  $\varphi$  is measured in a plane normal to the magnetic field.

Taking into account the explicit form of the velocity distribution function (2) and velocity space (5), it is easy to show that the particle and energy fluxes parallel to the magnetic field are zero. The particle density can be calculated by means of

$$n^{(B)}(\vec{r}) = \frac{4}{\sqrt{\pi}} n_0 \exp[-(U^2 + q)] \left\{ \int_0^{v_b} g_1(V) dV \int_0^{\frac{\pi}{2}} g_2(V, \theta) d\theta \right. \\ \left. + \int_{v_b}^{v_\infty} g_1(V) dV \int_0^{\theta_m} g_2(V, \theta) d\theta + \int_{v_\infty}^{v_c} g_1(V) dV \int_{\theta'_m}^{\theta_m} g_2(V, \theta) d\theta \right\} \quad , \quad (7)$$

in which the following notations are introduced

$$g_1(V) = V^2 \exp(-V^2) \quad ;$$

$$g_2(V, \theta) = \exp \left[ 2U(V^2 + q - \eta^{-1} V^2 \sin^2 \theta)^{1/2} \right] \sin \theta \quad ,$$

$$q = m R/2kT_0 \quad ,$$

$$Z = z(m/2kT_0)^{1/2} \quad ,$$

where z stands for u, v, v<sub>b</sub>, v<sub>∞</sub> and v<sub>c</sub>.

In order to reduce the double integrals to simple integrals we use the transformation

$$\begin{aligned} V &= (x^2 + y^2 - q)^{1/2} \\ \theta &= \arcsin \frac{\eta^{1/2} x}{(x^2 + y^2 - q)^{1/2}} \end{aligned} \quad (8)$$

which yields the Jacobian

$$\left| \frac{\partial(V, \theta)}{\partial(x, y)} \right| = \eta^{1/2} y (px^2 + y^2 - q)^{-1/2} (x^2 + y^2 - q)^{-1/2} \quad ,$$

with  $p = 1 - \eta$ .

Inserting this in (7) gives

$$n^{(B)}(\vec{r}) = \frac{4}{\sqrt{\pi}} n_0 \eta \exp(-U^2) \iint_{G_1} h(x, y) dx dy \quad , \quad (9)$$

with

$$h(x, y) = xy(px^2 + y^2 - q)^{-1/2} \exp[-(x^2 + y^2) + 2Uy] \quad , \quad (10)$$

and where the integration is to be taken over the region  $G_1$ , illustrated in Fig. 1.

Performing the x integration we finally obtain

$$n^{(B)}(\vec{r}) = 2n_0 \gamma [ H(0, A, S_1) - H(q^{1/2}, A, T_1) ] \quad , \quad (11)$$

where, for convenience, we used the shorthand notations

$$\begin{aligned} H(s, t, S) &= \int_s^t S(y) y \exp(\eta p^{-1} y^2 + 2Uy) dy \quad , \\ S_1 &= \text{erf} [ p^{-1/2} (X^2 + a\sigma\tau^{-1} y^2)^{1/2} ] \quad , \end{aligned} \quad (12)$$

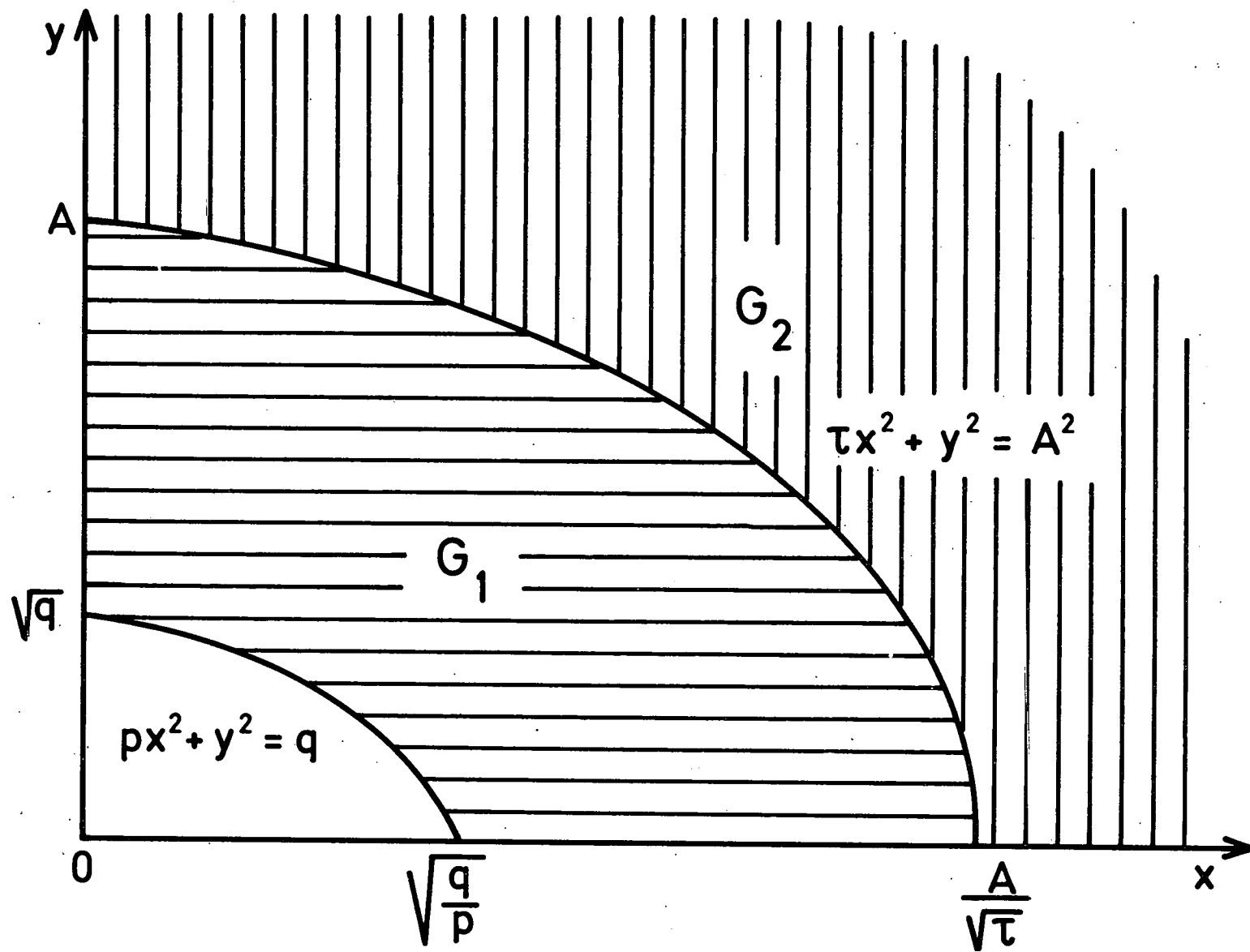


Fig. 1.- Domains of integration for the ballistic ( $G_1$ ) and escaping ( $G_2$ ) particles.

$$T_1 = \text{erf} [p^{-1/2} (y^2 - q)^{1/2}] ,$$

$$\tau = 1 - a \geq 0, \quad \sigma = \mu - 1 \geq 0 ,$$

$$A^2 = - \psi m(1 + a)/kT_0 \geq 0 ,$$

$$X^2 = - \psi m [(1 + \beta)y - a\sigma\tau^{-1} (1 + a)]/kT_0 ,$$

$$\gamma = \eta p^{-1/2} \exp [-(U^2 + qp^{-1})] ;$$

with the error-function  $\text{erf}(z)$  given by

$$\text{erf}(z) = \frac{2}{\sqrt{\pi}} \int_0^z e^{-t^2} dt.$$

Formula (11) gives the number density distribution for ballistic particles in the exosphere. The two functions  $H$  on the right hand side of (11) have to be evaluated by numerical integration.

To calculate the momentum fluxes we proceed in a quite similar way. The region of integration in the  $xy$  plane remains  $G_1$  since it is only determined by the velocity space (5). The function  $h(x,y)$  in (9), however, is determined by the moment of the velocity distribution. For the parallel and perpendicular momentum fluxes, for example, we have respectively,

$$h(x,y) = 2 kT_0 xy(px^2 + y^2 - q)^{1/2} \exp [-(x^2 + y^2) + 2Uy] ,$$

and

$$h(x,y) = kT_0 \eta x^3 y(px^2 + y^2 - q)^{-1/2} \exp [-(x^2 + y^2) + 2Uy] .$$

After some calculations we obtain :

(a) the parallel momentum flux

$$P_{\parallel}^{(B)}(\vec{r}) = 4 p_0 \gamma p [ H(0, A, S_2) - H(q^{1/2}, A, T_2) ] , \quad (13)$$

with  $p_0 = n_0 k T_0$ ,

$$S_2 = K_2 [p^{-1/2} (x^2 + a\sigma\tau^{-1}y^2)^{1/2}] ,$$

$$T_2 = K_2 [p^{-1/2} (y^2 - q)^{1/2}] .$$

The function  $K_2(z)$  is defined by

$$K_2(z) = \frac{2}{\sqrt{\pi}} \int_0^z t^2 e^{-t^2} dt ,$$

and can be expressed in terms of the error function and the exponential function<sup>1</sup>;

(b) the perpendicular momentum flux

$$P_{\perp}^{(B)}(\vec{r}) = 2 p_0 \gamma \eta [ H(O, A, S_3) - H(q^{1/2}, A, T_3) ] , \quad (14)$$

with

$$S_3 = S_2 - p^{-1}(y^2 - q) S_1 ,$$

$$T_3 = T_2 - p^{-1}(y^2 - q) T_1 .$$

### B. Escaping Particles

For this class of particles we have to make a difference between particles with a positive and a negative potential energy  $m R/2$ . Lemaire and Scherer<sup>1</sup> have shown that in the former case the velocities  $v$  and the pitch angles  $\theta$  are limited by the following inequalities

$$v_{\infty} \leq v \leq v_c , \quad 0 \leq \theta \leq \theta'_m ;$$

$$v_c \leq v < \infty , \quad 0 \leq \theta \leq \theta_m ;$$

so that the particle density can be calculated by means of

$$\begin{aligned} n^{(E)}(\vec{r}) = \frac{2}{\sqrt{\pi}} n_0 \exp[-(U^2 + q)] & \left\{ \int_{v_{\infty}}^{v_c} g_1(v) dv \int_0^{\theta'_m} g_2(v, \theta) d\theta \right. \\ & \left. + \int_{v_c}^{\infty} g_1(v) dv \int_0^{\theta_m} g_2(v, \theta) d\theta \right\} . \end{aligned} \quad (15)$$

Taking into account transformation (8), expression (15) can be reduced to

$$n^{(E)}(\vec{r}) = \frac{2}{\sqrt{\pi}} n_0 \eta \exp(-U^2) \iint_{G_2} h(x,y) dx dy, \quad (16)$$

where the region of integration  $G_2$  is shown in Fig. 1, and the integrand  $h(x,y)$  is defined in (10).

The double integral on the right hand side of (16) can be reduced to two simple integrals which yields

$$n^{(E)}(\vec{r}) = n_0 \gamma [ H(o,A,S_4) + H(A,\infty,T_4) ] \quad , \quad (17)$$

with

$$S_4 = 1 - S_1 \quad ,$$

$$T_4 = 1 - T_1 \quad .$$

Similar calculations give :

(a) the parallel momentum flux

$$P_{\parallel}^{(E)}(\vec{r}) = 2 p_0 \gamma p [ H(o,A,S_5) + H(A,\infty,T_5) ] \quad , \quad (18)$$

with

$$S_5 = 0.5 - S_2 \quad ,$$

$$T_5 = 0.5 - T_2 \quad ;$$

(b) The perpendicular momentum flux

$$P_{\perp}^{(E)}(\vec{r}) = p_0 \gamma \eta [ H(o,A,S_6) + H(A,\infty,T_6) ] \quad (19)$$

with

$$S_6 = S_5 - p^{-1}(y^2 - q) S_4 \quad ,$$

$$T_6 = T_5 - p^{-1}(y^2 - q) T_4 \quad .$$

To determine the particle and energy fluxes we can still use the transformation (8) where the integration over the region  $G_2$  can now be performed analytically. The corresponding moments of the velocity distribution, however, can also be calculated straightforward. For the particle flux this yields

$$F^{(E)}(\vec{r}) = \frac{1}{4} n_0 c \eta (W + X - Y + Z) \quad , \quad (20)$$

with

$$c = (8kT_0/\pi m)^{1/2} \quad ,$$

$$W = a^{-1} \exp [ - (A - U)^2 ] \quad ,$$

$$X = \sqrt{\pi} U \operatorname{erfc} (A - U) \quad , \quad (21)$$

$$Y = a^{-1} \tau \exp [ - (\tau^{-1} A^2 + U^2) ] \quad ,$$

$$Z = \sqrt{\pi} U (\tau/a)^{3/2} [ D(a^{-1/2} \tau^{1/2} U) - D(a^{1/2} \tau^{-1/2} A + a^{-1/2} \tau^{1/2} U) ] \\ \times \exp [ - (\tau^{-1} A^2 + a^{-1} U^2) ] \quad .$$

The complementary error function and Dawson's integral are respectively defined by

$$\operatorname{erfc}(z) = \frac{2}{\sqrt{\pi}} \int_z^\infty \exp(-t^2) dt = 1 - \operatorname{erf}(z) \quad ,$$

and

$$D(z) = \frac{2}{\sqrt{\pi}} \int_0^z \exp(t^2) dt \quad .$$

On the other hand we can calculate the energy flux by means of

$$\epsilon(\vec{r}) = \frac{1}{4} p_0 c \eta \left\{ [ 2 - q + (1 - a^{-1} \tau) U^2 + UA + A^2 ] W + (U^2 - q + 2.5) X \right. \\ \left. - PY + (P + 0.5) Z \right\} \quad , \quad (22)$$

where P stands for

$$P = 2 - q - a^{-1} \tau U^2 + \tau^{-1} A^2 \quad .$$

For escaping particles with a negative potential energy it was shown<sup>1</sup> that the velocity space is determined by

$$(-R)^{1/2} \leq v < \infty \quad , \quad 0 \leq \theta \leq \theta_m \quad , \quad 0 \leq \varphi < 2\pi \quad .$$

Applying the transformation (8), the particle density is given by

$$n^{(E)}(\vec{r}) = \frac{2}{\sqrt{\pi}} n_0 \eta \exp(-U^2) \int_0^\infty dy \int_0^\infty h(x,y) dx, \quad (23)$$

where  $h(x,y)$  is defined in (10).

The right hand side of (23) is a special case ( $A = 0$ ) of the double integral in (16). By making the formal substitution  $A = 0$ , we can immediately derive the formulae which give the macroscopic quantities for particles with a negative potential energy, from the corresponding expressions derived for the escaping particles with a positive potential energy.

#### IV. NUMERICAL RESULTS

It is easy to check that for  $u \rightarrow 0$ , the formulae deduced in Sec. III, reduce to the corresponding expressions, given by Lemaire and Scherer<sup>1</sup>. To exhibit the influence of an asymmetry in the velocity distribution of the particles in the terrestrial polar ion-exosphere we consider an ( $O^+ - H^+ - e$ ) - exosphere with a vanishing magnetic field at infinity. Moreover, we use a dipole configuration for the terrestrial magnetic field up to a radial distance of about four Earth radii. The baropause is chosen at 2000 km above the polar cap, the ion and electron temperatures at this level are 3000°K, and the concentrations are  $n_e(r_0) = 10^3 \text{ cm}^{-3}$ ,  $n_{O^+}(r_0) = 9 \times 10^2 \text{ cm}^{-3}$ , and  $n_{H^+}(r_0) = 10^2 \text{ cm}^{-3}$ . Furthermore, we take a symmetric Maxwellian velocity distribution for the oxygen ions ( $u_{O^+} = 0$ ) since their effusion velocity is very small compared with the  $O^+$  mean thermal speed [ $w_{O^+}(r_0)/c_{O^+} \cong 10^{-9}$ ]. The effect of an asymmetry in the electron velocity distribution (corresponding with parameter values  $u_e \leq 10 \text{ km sec}^{-1}$ ) is also negligible [ $w_e(r_0)/c_e \cong 10^{-3}$ ]. Therefore, we confine ourselves to the study of the influence of an asymmetric proton velocity distribution.

In what follows we considered three values of the parameter  $u_{H^+}$ , i.e., 0,5, and  $10 \text{ km sec}^{-1}$ . We computed the macroscopic quantities calculated in Sec. III along a magnetic field line which intersects the baropause at a geomagnetic latitude of  $80^\circ$ . The results do not differ significantly with the choice of the open field line. Moreover, we neglect the incoming particles, and assume that the trapped electrons and oxygen ions are in thermal equilibrium, respectively, with the electron and  $O^+$  emerging from the barosphere. The number density and momentum fluxes for these trapped particles were determined in a previous paper<sup>1</sup>, to which we also refer for a detailed description of the method of computation.

Table I gives the values of the effusion velocity or bulk velocity  $w_{H^+}(r_0)$  and the escape flux  $F_{H^+}(r_0)$  of the hydrogen ions at the baropause. The bulk velocity is always larger than  $u_{H^+}$ . Only for unreasonably high asymmetric velocity distribution functions, does  $w_{H^+}(r_0)$  become nearly equal to  $u_{H^+}$ . The escape flux of the protons increases with  $u_{H^+}$  since in the three models we assumed the same concentrations at the baropause level.

The reduced potential energy  $mR/2kT_0$  is plotted for each species in Fig. 2, which shows that for growing values of the parameter  $u_{H^+}$ , the total potential energy  $mR/2$  increases for the ions but decreases for the electrons. Qualitatively, however, there is no difference from the results obtained with a symmetric proton velocity distribution (represented by a solid line): The electrons and oxygen ions have a monotonic increasing positive potential energy distribution and therefore are decelerated. The protons on the contrary are blown out since they have a monotonic decreasing negative potential energy. The escape flux of the thermal electrons is determined by the electric potential difference between the baropause and infinity. Moreover, the electron flux will be equal to the proton flux because the escape of oxygen ions is negligible. Since the proton flux increases with  $u_{H^+}$ , the electron escape flux will also increase and therefore the potential barrier which the escaping electrons have to overcome, must decrease.

Figure 3 illustrates how the electric field intensity in the exosphere diminishes with increasing  $u_{H^+}$ . As a consequence the acceleration of the ions is also reduced. Therefore, although the effusion velocity at the baropause increases significantly with  $u_{H^+}$ , the bulk velocity at high altitudes is not much different from the constant value corresponding to a symmetric velocity distribution function. This is shown in Fig. 4 where we plotted the bulk velocity of the protons in  $\text{km sec}^{-1}$  (left hand scale) and of the oxygen ions in  $\text{cm sec}^{-1}$  (right hand scale).

The ion number densities versus altitude are given in Fig. 5. Note that although  $n_{H^+}$  increases and  $n_{O^+}$  decreases for an increasing asymmetry in the velocity distribution function, the scale height is practically not affected above 6000 km in altitude.

In Fig. 6 we illustrate the average temperature and the temperature anisotropy distributions. For the oxygen ions the temperature is nearly independent of  $u_{H^+}$  and remains

TABLE I : Effusion velocity ( $w_{H^+}$ ) and escape flux ( $F_{H^+}$ ) at the baropause for different degrees of asymmetry ( $u_{H^+}$ ) in the proton velocity distribution.

$u_{H^+}$ km sec <sup>-1</sup>	$u_{H^+}/c_{H^+}$	$w_{H^+}(r_0)$ km sec <sup>-1</sup>	$w_{H^+}(r_0)/c_{H^+}$	$F_{H^+}(r_0)$ cm <sup>-2</sup> sec <sup>-1</sup>
0	0	4.0	0.5	$4.0 \times 10^7$
5	0.6	6.3	0.8	$6.3 \times 10^7$
10	1.2	10.3	1.3	$1.0 \times 10^8$

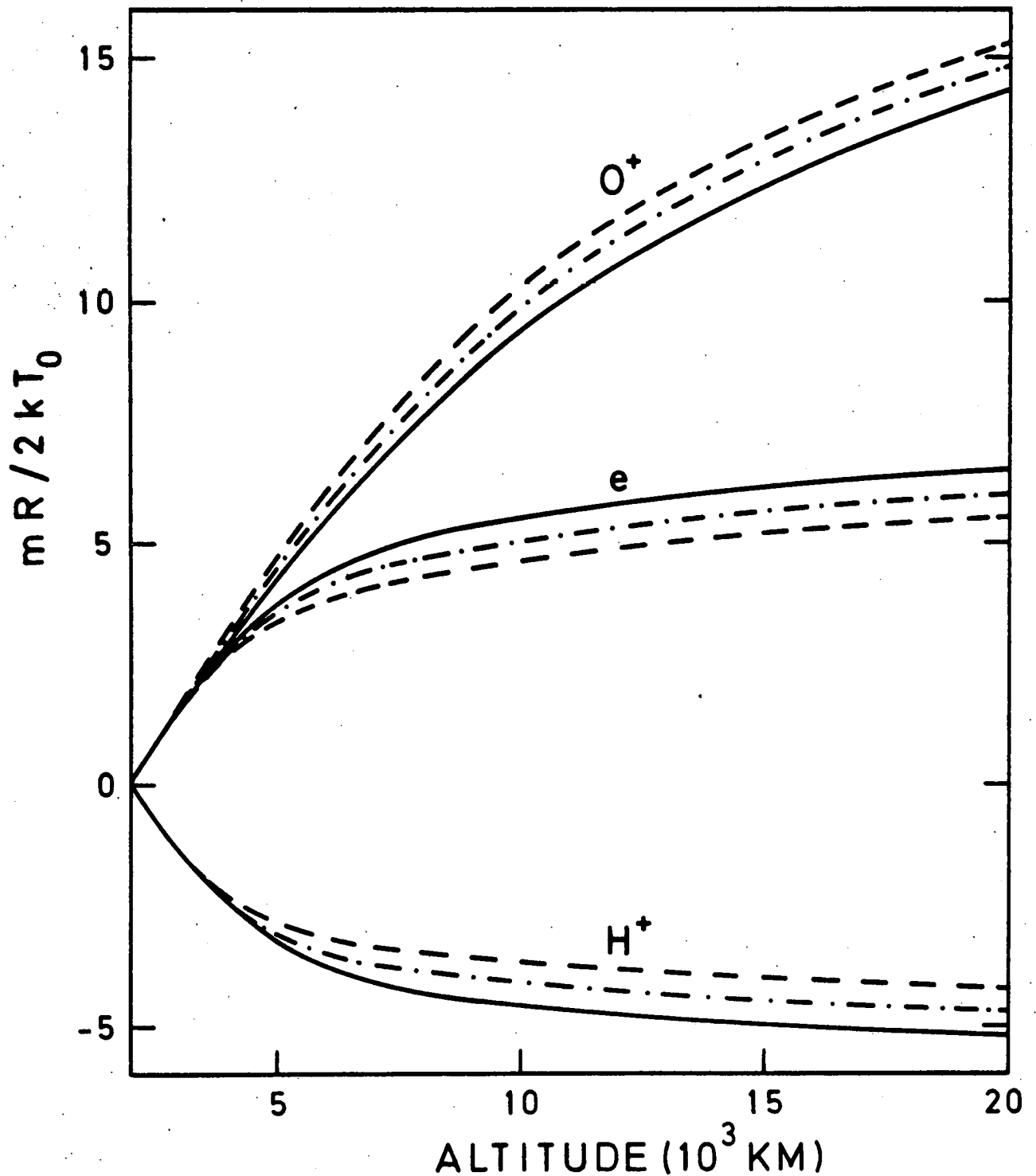


Fig. 2.- Reduced potential energies versus altitude along a magnetic field line crossing the baropause (2000 km altitude) at  $80^\circ$  latitude. At the baropause each species has a temperature of  $3000^\circ\text{K}$ , and the concentrations are  $n_e = 10^3 \text{ cm}^{-3}$ ,  $n_{O^+} = 9 \times 10^2 \text{ cm}^{-3}$ , and  $n_{H^+} = 10^2 \text{ cm}^{-3}$ . The solid, the dot-dashed, and the dashed lines, respectively correspond to the values of the parameter  $u_{H^+} = 0, 5, \text{ and } 10 \text{ km sec}^{-1}$ .

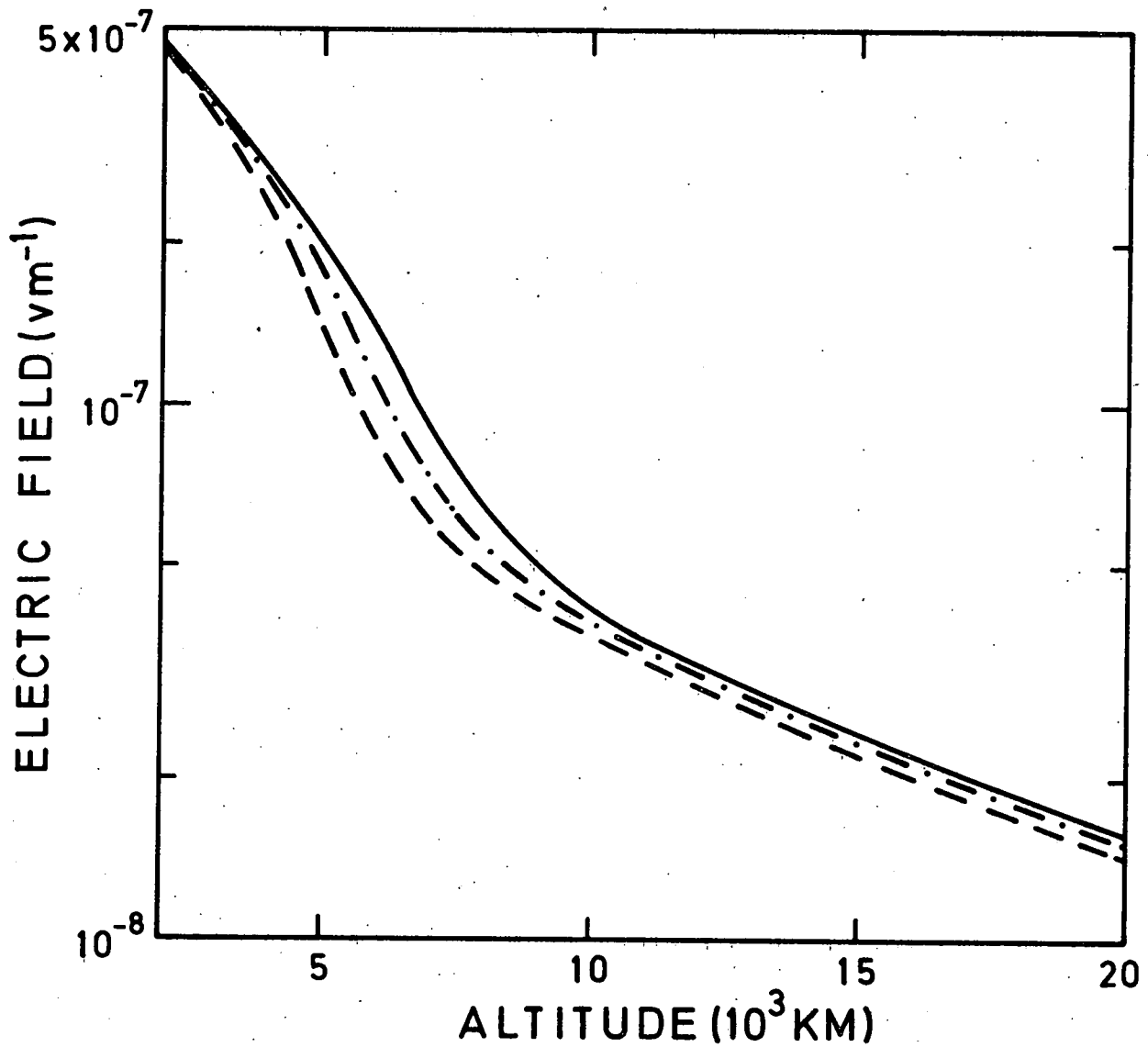


Fig. 3.- The electric field distribution along a magnetic field line crossing the baropause (2000 km altitude) at 80° latitude. At the baropause the ion and electron temperatures are 3000°K, and the concentrations are  $n_e = 10^3 \text{ cm}^{-3}$ ,  $n_{O^+} = 9 \times 10^2 \text{ cm}^{-3}$ , and  $n_{H^+} = 10^2 \text{ cm}^{-3}$ . The solid, the dot-dashed, and the dashed line respectively correspond to the values of  $u_{H^+} = 0.5, \text{ and } 10 \text{ km sec}^{-1}$ .

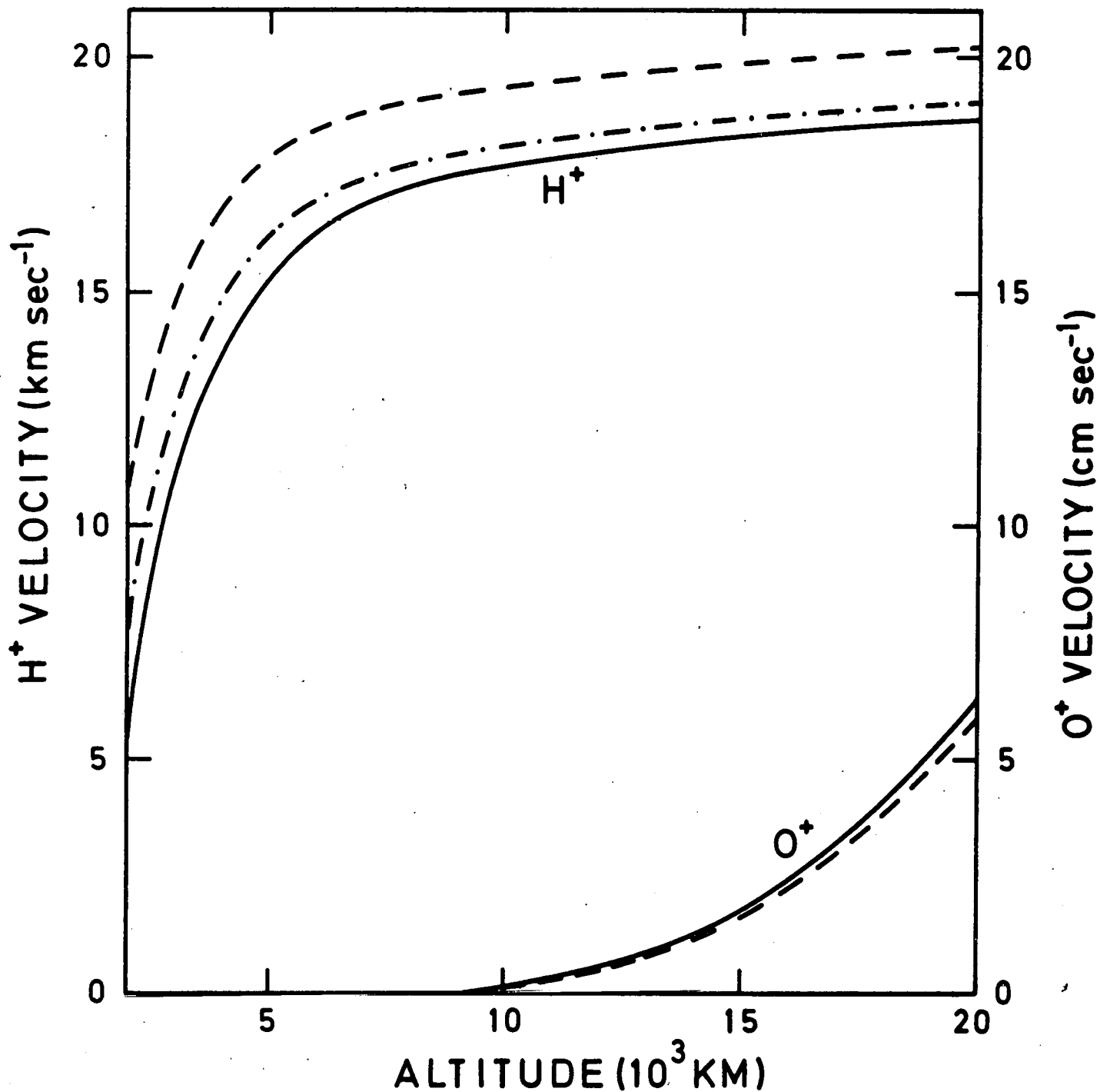


Fig. 4.- The bulk velocity versus altitude along a magnetic field line crossing the baropause (2000 km altitude) at  $80^\circ$  latitude. At the baropause the ion and electron temperatures are  $3000^\circ\text{K}$ , and the concentration are  $n_e = 10^3 \text{ cm}^{-3}$ ,  $n_{\text{O}^+} = 9 \times 10^2 \text{ cm}^{-3}$ , and  $n_{\text{H}^+} = 10^2 \text{ cm}^{-3}$ . The solid, the dot-dashed, and the dashed lines respectively correspond to the values of  $u_{\text{H}^+} = 0,5$  and  $10 \text{ km sec}^{-1}$ .

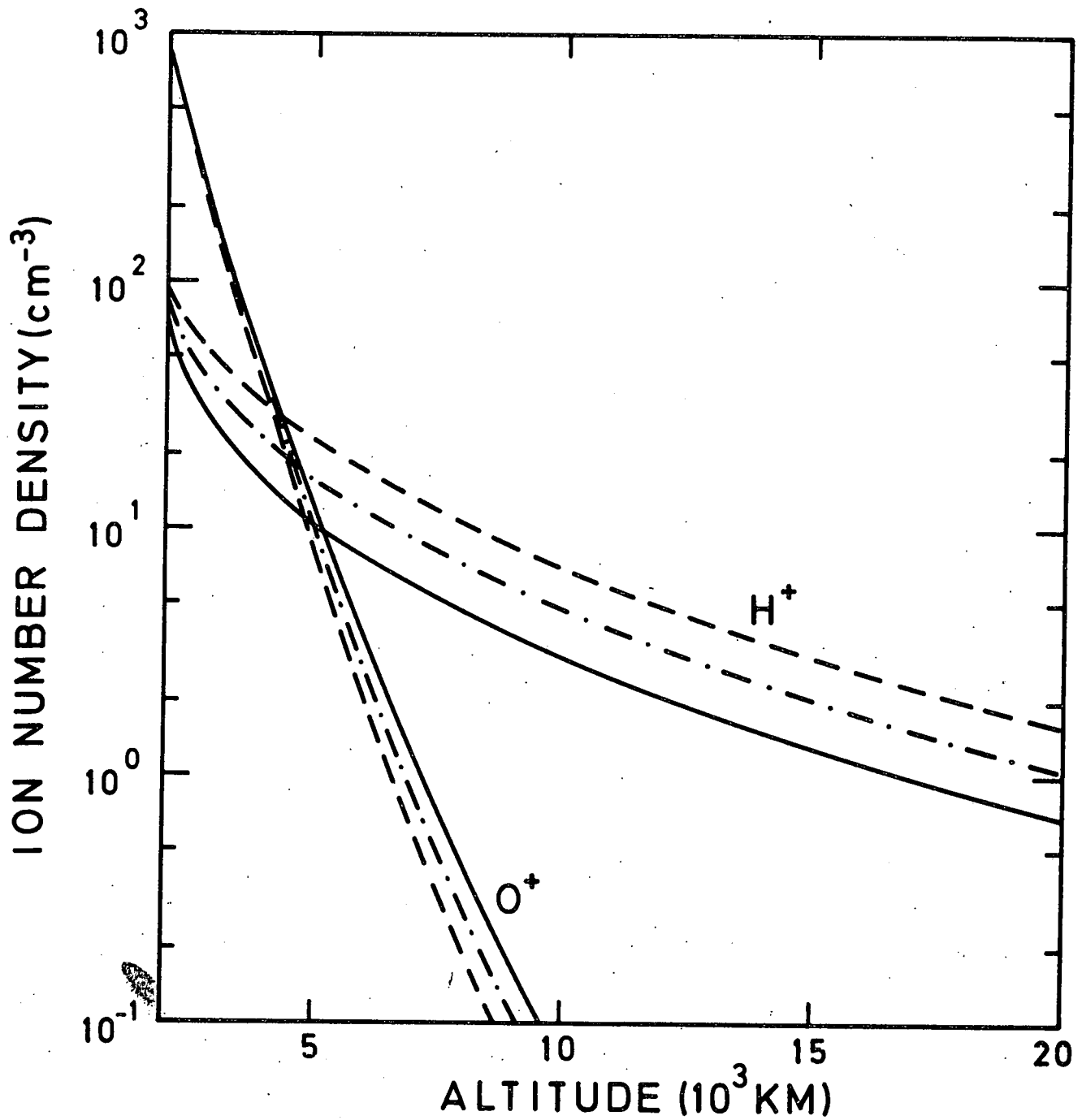


Fig. 5.- The ion number densities versus altitude along a magnetic field line crossing the baropause (2000 km altitude) at 80° latitude. At the baropause each species has a temperature of 3000°K, and the concentrations are  $n_e = 10^3 \text{ cm}^{-3}$ ,  $n_{O^+} = 9 \times 10^2 \text{ cm}^{-3}$ , and  $n_{H^+} = 10^2 \text{ cm}^{-3}$ . The solid, the dot-dashed, and the dashed lines, respectively, correspond to the values of  $u_{H^+} = 0.5$  and  $10 \text{ km sec}^{-1}$ .

practically constant and isotropic. The electron temperature decreases slightly and the growth of the anisotropy is very small for an increasing asymmetry of the proton velocity distribution. The effect upon the hydrogen average temperature and temperature anisotropy, however, is much more pronounced ; both become larger with increasing values of  $u_{H^+}$ .

Finally, we give the proton and electron conduction flux versus altitude in Fig. 7, which shows growth with an increasing degree of asymmetry for both constituents. The electron conduction flux is approximately two orders of magnitude larger than the conduction flux of the ions, which is practically equal to the proton conduction flux.

#### *V. CONCLUSIONS*

Although a reasonable value of the parameter  $u_{H^+}$  will probably not exceed a small fraction of the thermal speed, we considered the influence of very large asymmetries in the velocity distribution function at the baropause. The results presented above, show that for the terrestrial polar ion-exosphere, the most salient properties are qualitatively not affected by considering such an asymmetry; i.e., (1) the protons are accelerated outwardly by a small electric field which retains the electrons. (2) the proton flow speed rapidly becomes supersonic, but the oxygen ions are bound to the Earth by the gravitational force which is larger than the electric force.

#### *ACKNOWLEDGMENT*

We appreciate the valuable advice and continuous interest of Prof. Dr. M. NICOLET during the preparation of this work.

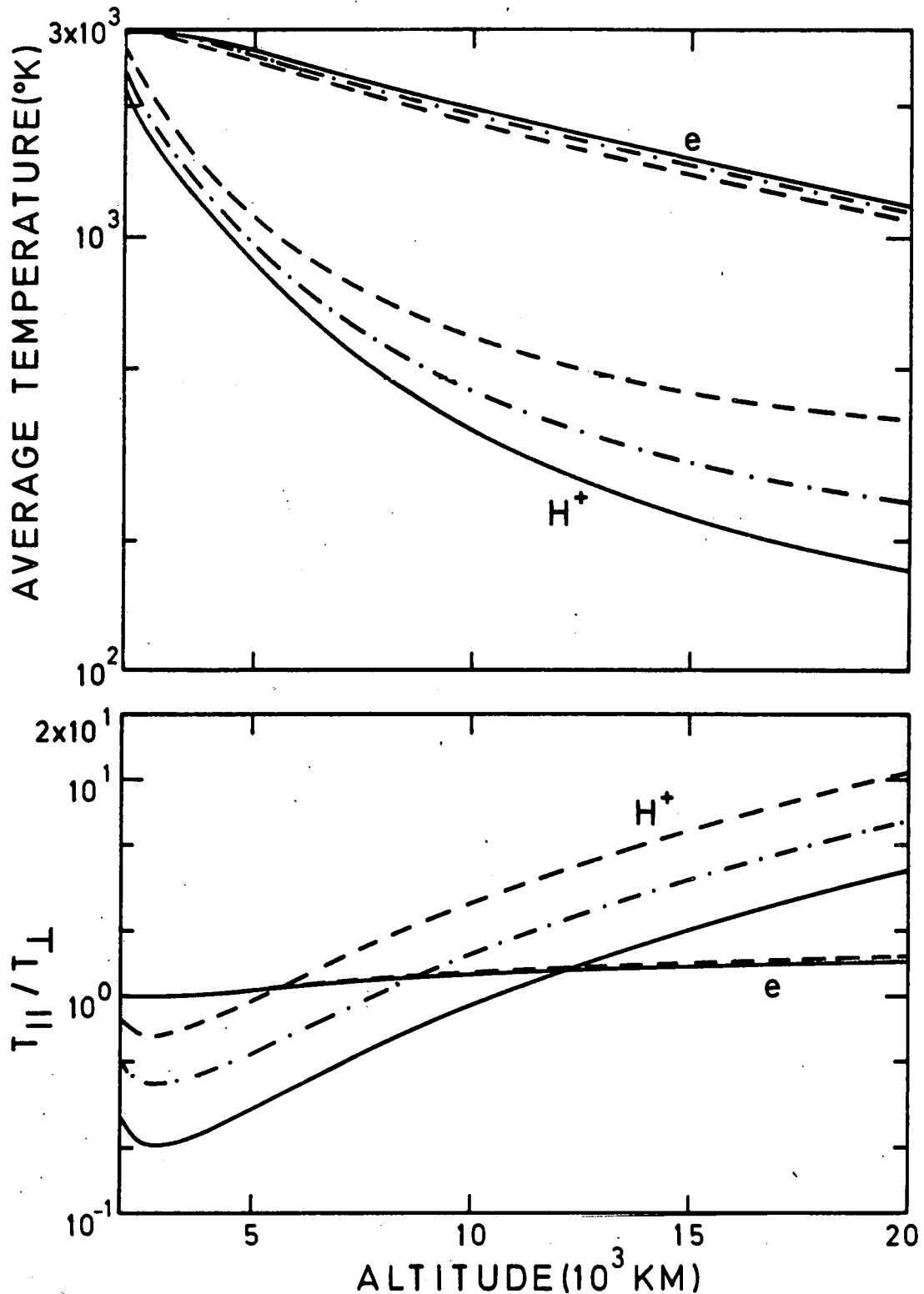


Fig. 6.- The average temperatures and temperature anisotropies versus altitude along a magnetic field line crossing the baropause (2000 km altitude) at  $80^\circ$  latitude. At the baropause each species has a temperature of  $3000^\circ\text{K}$ , and the concentrations are  $n_e = 10^3 \text{ cm}^{-3}$ ,  $n_{O^+} = 9 \times 10^2 \text{ cm}^{-3}$ , and  $n_{H^+} = 10^2 \text{ cm}^{-3}$ . The solid, the dot-dashed, and the dashed lines respectively correspond to the values of  $u_{H^+} = 0,5$  and  $10 \text{ km sec}^{-1}$ .

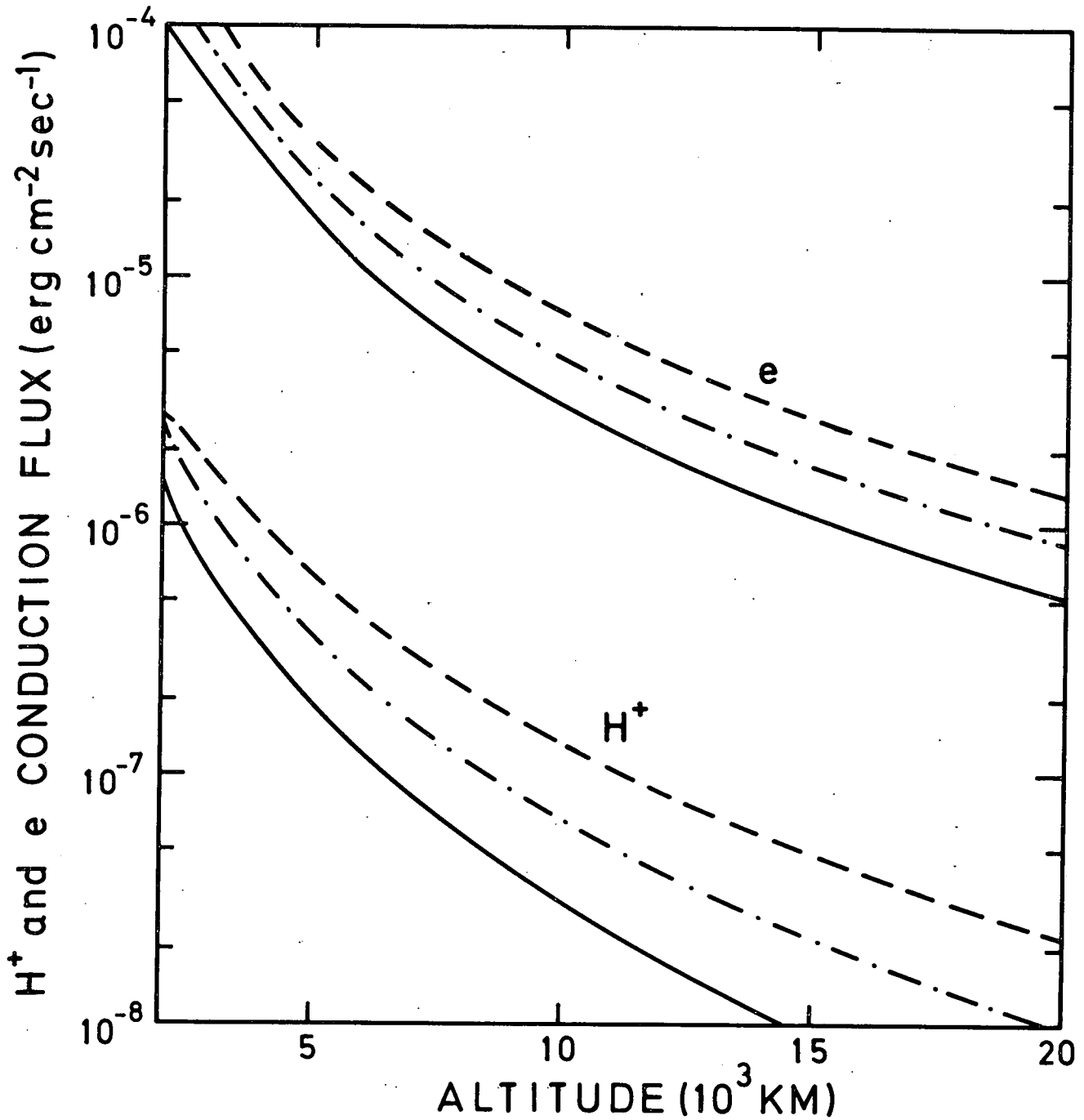


Fig. 7.- The conduction flux distributions along a magnetic field line crossing the baropause (2000 km altitude) at  $80^\circ$  latitude. At the baropause the ion and electron temperatures are  $3000^\circ\text{K}$ , and the concentrations are  $n_e = 10^3 \text{ cm}^{-3}$ ,  $n_{O^+} = 9 \times 10^2 \text{ cm}^{-3}$ , and  $n_{H^+} = 10^2 \text{ cm}^{-3}$ . The solid, the dot-dashed and the dashed lines, respectively correspond to the values of  $u_{H^+} = 0.5$ , and  $10 \text{ km sec}^{-1}$ .

## REFERENCES

1. J. LEMAIRE and M. SCHERER, *Phys. Fluids*, **14**, 1683 (1971).
2. J. LEMAIRE and M. SCHERER, *Planet. Space Sci.*, **18**, 103, (1970).
3. P.M. BANKS and T.E. HOLZER, *J. Geophys. Res.*, **73**, 6846 (1968).
4. P.M. BANKS and T.E. HOLZER, *J. Geophys. Res.*, **74**, 6317 (1969).
5. J.H. HOFFMAN, *Int. J. Mass. Spectrom. Ion Phys.*, **4**, 315 (1970).
6. K. MARUBASHI, *J. Radio Res. Lab.*, **17**, 335 (1970).
7. K. MARUBASHI, *Rep. Ionos. Space Res. (Japan)*, **24**, 323 (1970).
8. T.E. HOLZER, J.A. FEDDER, and P.M. BANKS, *J. Geophys. Res.*, **76**, 2453 (1971).